Conformational Analysis of Poly(*N*-vinylcarbazole) by NMR Spectroscopy and Molecular Modeling

Aglaia Karali and Photis Dais*

NMR Laboratory, Department of Chemistry, University of Crete, 71409 Iraklion, Crete, Greece

Emmanuel Mikros

Department of Pharmacy, Division of Pharmaceutical Chemistry, University of Athens, 15771 Athens, Greece

Frank Heatley

Department of Chemistry, University of Manchester, Manchester M13 9PL, U.K.

Received January 22, 2001

ABSTRACT: NOESY experiments and molecular mechanics calculations have been used to examine the solution conformation of the synthetic polymer poly(*N*-vinylcarbazole) (PNVC). The diagonal and cross-peak volumes of theoretical NOESY spectra have been calculated for several mixing times by employing the complete relaxation matrix analysis (CORMA) introducing as structural models for the polymer chain conformation the triad stereochemical sequences (isotactic, heterotactic, and syndiotactic). Comparison between measured volumes and volumes calculated from the proposed structures allowed an assessment of the validity of the model structures. The data do not support a single conformational model, and only conformational averaging between different model structures can provide satisfactory agreement between theoretical and experimental parameters. On the basis of the conformational preference of the bulky carbazole groups of PNVC in the various stereochemical sequences, some useful conclusions were derived in relation to the photophysical behavior of this commercial polymer.

Introduction

The photophysical properties of poly(*N*-vinylcarbazole) (PNVC) (**1**) are unique among vinyl aromatic

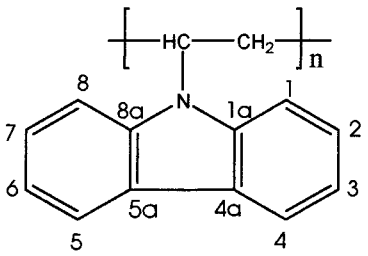

1

polymers. Time-resolved fluorescence studies[1−4] of PNVC reveal the formation of two distinct excimers: a sandwich type, the so-called true excimer, with maximum wavelength near 420 nm, and a second excimer near 370 nm. The first excimer is formed when two carbazole groups have achieved an eclipsed, sandwich-like conformation, whereas for the formation of the second excimer a partial overlap of two carbazole groups has been invoked. The formation of the second excimer is associated with syndiotactic stereochemical sequences in the polymer chain. Emission from the true excimer is relatively more intense in a more isotactic polymer. Apparently, tacticity is an important factor in the relative abundance of these two types of excimers.[3,4]

The influence of the local chain motions of PNVC on the excimer formation has been considered in a previous publication.[5] It was concluded that the segmental motion of the polymer backbone, but not the side-chain motion, influences the excimer formation. The ^{13}C NMR relaxation data of the protonated aromatic carbons of the carbazole group showed that the internal motion of the carbazole group about the C−N bond is highly restricted.

Although tacticity and segmental dynamics of PNVC appear to be important factors for the formation of the two types of excimers mentioned previously, the relative orientation of two carbazole groups is also a crucial factor which determines the appropriate disposition of two pendant chromophores and the formation of excimers. On the basis of ^1H NMR spectroscopy[6−9] and time-resolved fluorescence spectra in the picosecond and nanosecond time scale[3,7−9] of model compounds *meso* and *racemic* 2,4-dicarbazolylpentane, it has been proposed that the second excimer results from the most stable ground-state tt conformation of a syndiotactic dyad, which is the precursor of the tt excimer, with partial overlap of the carbazole rings. A small conformational change (∼20°) is adequate to induce the second excimer emission. Thus, the formation of the second excimer is very fast (less than 2 ns) and is characterized by a low activation energy. Further rotation to a full overlap of the neighboring chromophores is sterically prohibited. The true excimer is formed in several nanoseconds and requires a 120° rotation about the C−C bond of an isotactic dyad. This bond rotation brings two carbazole rings from the most stable ground tg (or gt) state conformation of the *meso* dyad to the tt excimer state where they are totally overlapped. Thus, the magnitude of the activation energy of the sandwich-like excimer formation is expected to be similar to barriers to rotational motion about C−C bonds in alkanes.

* To whom correspondence should be addressed. E-mail dais@chemistry.uch.gr.

10.1021/ma010117n CCC: $20.00
Published on Web 07/03/2001

Although the experimental data on the pentane model prove the necessity to consider the different conformational behavior of the ground and excited states within the two dyads, the conformational distribution of a dyad in the polymer chain must be different from the conformational distribution in the corresponding models. For instance, theoretical calculations[6,10] indicate a higher population of the tt conformation in both the syndio and isotactic dyads in the polymer chain. This means that the excimer formation in the isotactic dyad will differ from the excimer formation in the *meso* dyad of the model compound, since the latter gives no indication of a contribution from the tt conformation. Another factor that is expected to influence the excimer formation in real chains is the presence of longer stereochemical sequences of the monomer units (triads, tetrads, pentads, etc.). In addition to syndiotactic and isotactic sequences, the microstructure of PNVC contains heterotactic sequences as shown by its proton and carbon NMR spectra.[11,12] The conformational energies of these longer sequences are expected to be different from each other and from those of the dyad sequences. Moreover, the highly restricted internal rotations of the carbazole side groups about the N−C bonds[5] do not guarantee that two carbazole groups will obtain the appropriate relative spatial disposition for excimer formation. Therefore, it is important to study the conformational behavior of real PNVC chains to draw conclusions about the excimer formation as reflected in the photophysical experiments.

In recent years, two-dimensional nuclear Overhauser enhancement (2D NOE or NOESY) spectra have been used in combination with geometry and energy refinement calculations to determine biomolecular structures in solution.[13,14] These experiments are based on proton−proton dipolar relaxation yielding a correlation map between protons of close proximity (≤6 Å). The intensities of the cross-peaks of the NOESY spectrum are related to the distances between the protons (the proton−proton cross-relaxation rates depend on the sixth power of the reciprocal of the distance) and can, therefore, be used to estimate these distances.

The present study describes the conformational behavior of this commercially important polymer as assessed by phase-sensitive NOESY experiments at different mixing times and the calculation of the peak intensities (or volumes) by using the method of the complete relaxation matrix analysis (CORMA).[15,16] The critical feature of CORMA is the explicit treatment of the relaxation network and in particular spin diffusion while calculating the NOESY intensities.

It should be noted that an alternative approach to analyzing the NOESY data is the so-called isolated spin pair approximation (ISPA).[17] This widely used method assumes that at short mixing times a cross-peak intensity correlating a particular proton−proton pair depends on the distance separating that pair alone. This assumption leads to the qualitative or semiquantitative extraction of interproton distances of the particular proton pairs. This method has not been used in the present study, since its validity has been questioned for practical applications.[18]

Experimental Section

NMR Spectroscopy. Proton spectra were obtained using a Bruker Spectrospin AMX spectrometer operating at 500 MHz. The data set were transferred to a personal computer for data processing using the program WINNMR (Bruker).

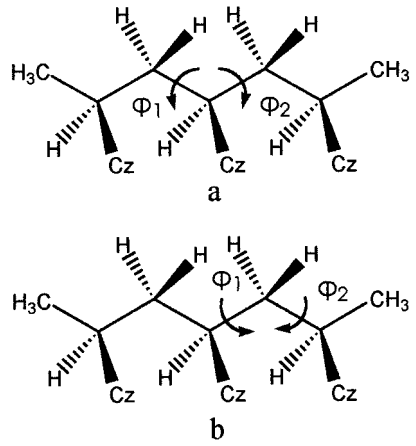

Figure 1. Structure of the model compound *meso* 2,4,6-tricarbazolylheptane in the all-trans conformation and designation of the torsional angles φ_1 and φ_2. (a) Rotations around the central bonds flanking the central carbazole group of the trimer. (b) Rotations around the penultimate bonds in the trimer. The angles φ_1 and φ_2 were rotated by 10° increments over the whole angular range (360°).

Phase-sensitive ^{1}H NOESY spectra were recorded in the TPPI mode using the $(90°-t_1-90°-\tau_m-90°-\text{acquire})_n$ pulse sequence[19] and several mixing times $\tau_m = 50$, 100, 150, 250, 350, 450, 550, 650, and 750 ms in order to trace accurately the time course of the proton magnetization caused by cross-relaxation (NOE buildup rates). The relaxation delay was set to 2.0 s. A total of 512 complex t_1 points were acquired, and the spectra were zero filled to a final size of 2K × 2K. A $\pi/2$ shifted sine-squared weighting function was applied prior to Fourier transformation. The peak volumes were measured using the software AURELIA provided by Bruker, which sums the intensity in the area around the peak of interest. The total volumes of the CH and CH_2 cross-peaks were measured despite the fact that these peaks are split into components due to tacticity. Nevertheless, tacticity has been taken into consideration while analyzing the NOESY spectra.

PNVC was purchased from Aldrich and purified by several reprecipitations from THF solvent using methanol as precipitant. Samples of 0.5 mmol/mL (based on the repeat unit) in chloroform-*d* solutions were used for the NOESY experiments. The probe temperature was 30 ± 1 °C as measured by precalibrated thermocouples in the probe insert.

Conformational Analysis. The analysis began by optimizing the geometry of the monomer *N*-ethylcarbazole by using the HyperChem 5.1 software.[20] The optimized geometry of the carbazole group was used in the subsequent optimization and intramolecular energy calculations of the *meso*, *racemic*, and *hetero* 2,4,6-tricarbazolylheptanes, which serve as model structures for the PNVC triad sequences (mm), (rr), and (mr), respectively. Intramolecular energy calculations were performed using the MM^+ molecular mechanics program incorporated in the HyperChem 5.1 software. Intramolecular energies for each model structure were calculated upon rotation around the central bonds flanking the central carbazole group of the trimer (Figure 1a), while the end carbazole groups were considered as rigid. The angles φ_1 and φ_2 were rotated by 10° increments over the whole angular range (360°). At each 10° step of angles rotations unconstrained MM^+ minimization was performed to calculate the energies associated with that pair of angles. This procedure classifies the various local (and global) minima on the potential energy surface.

The energies were calculated using a combination of an exponential repulsion term with an attractive $1/R^6$ dispersion interaction. The basic parameters are a van der Waals radious r_i* for each atom type and a hardness parameter, ϵ_i, that determines the depth of the attractive well and the easiness by which atoms are pushed together. The torsional energy interaction involves three terms of 1-fold, 2-fold, and 3-fold symmetry with a phase angle of $\varphi_0 = 0$ and barriers heights

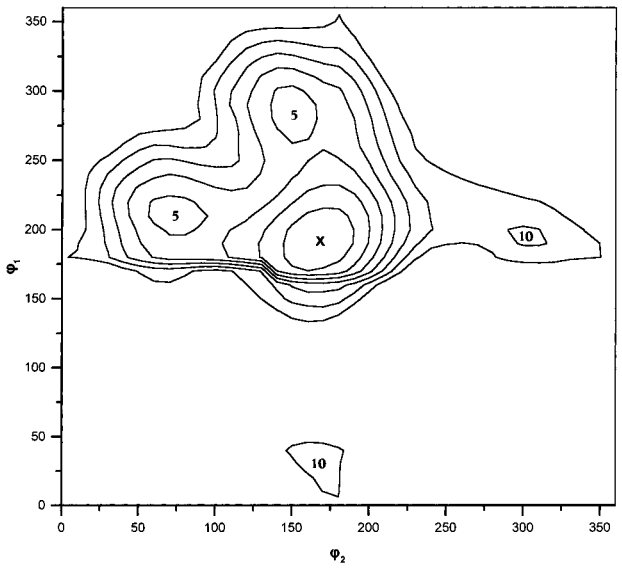

Figure 2. Conformational energy map, in kcal mol^{-1}, for the *meso* 2,4,6-tricarbazolylheptane corresponding to the isotactic triad (mm). The energies are expressed relative to the global minimum denoted by the × symbol.

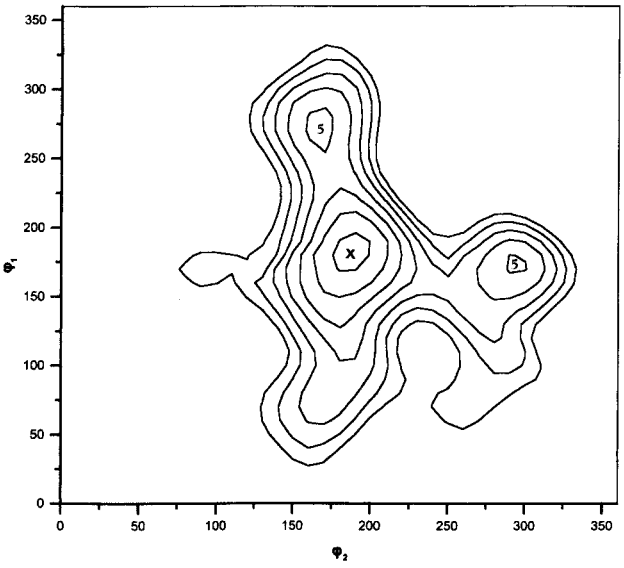

Figure 3. Conformational energy map, in kcal mol^{-1}, for the *recemic* 2,4,6-tricarbazolylheptane corresponding to the syndiotactic triad (rr). The energies are expressed relative to the global minimum denoted by the × symbol.

of 0.20, 0.27, and 0.093 kcal mol^{-1}, respectively. The energy of the deformation of the valence angle θ from its normal value θ_0 was estimated through a harmonic function $V(\theta) = K_\theta(\theta - \theta_0)^2$, where K_θ is half of the force constant. Calculations were performed without taking into account solute−solvent interactions, while for electrostatic interactions the bond-dipole option of the program was used. No rotations of the carbazole groups were considered in these calculations. As noted previously, internal motion of the carbazole group about the C−N bond is highly restricted.

Conformational energy maps obtained from these calculations are shown in Figures 2, 3, and 4 for the *meso*, *racemic*, and *hetero* 2,4,6-tricarbazolylheptanes, respectively. As can be seen in these figures, three energy minima are observed for each structure. The global minima (denoted by × symbols) correspond to the pair of angles $\varphi_1 = 162°$ and $\varphi_2 = 198°$ for the *meso* trimer, $\varphi_1 = 180°$ and $\varphi_2 = 177°$ for the *racemic* trimer, and $\varphi_1 = 162°$ and $\varphi_2 = 174°$ for the *hetero* trimer. Figure 5 depicts the structures of the three trimers, which correspond to the energy minima in Figures 2−4. The relative

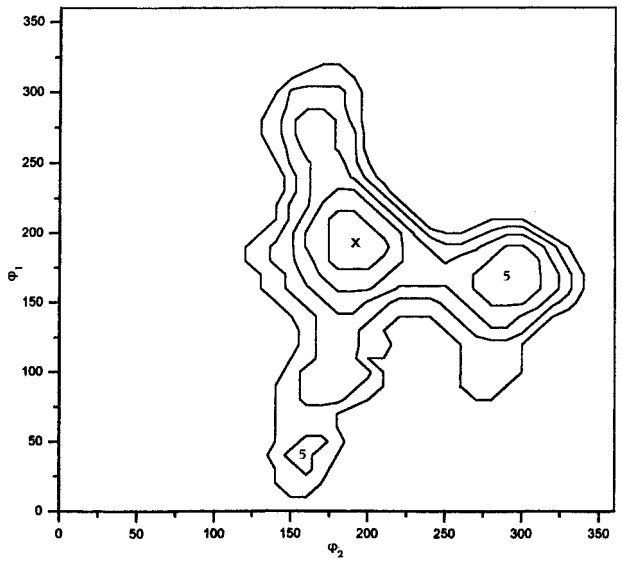

Figure 4. Conformational energy map, in kcal mol^{-1}, for the *hetero* 2,4,6-tricarbazolylheptane corresponding to the heterotactic triad (mr). The energies are expressed relative to the global minimum denoted by the × symbol.

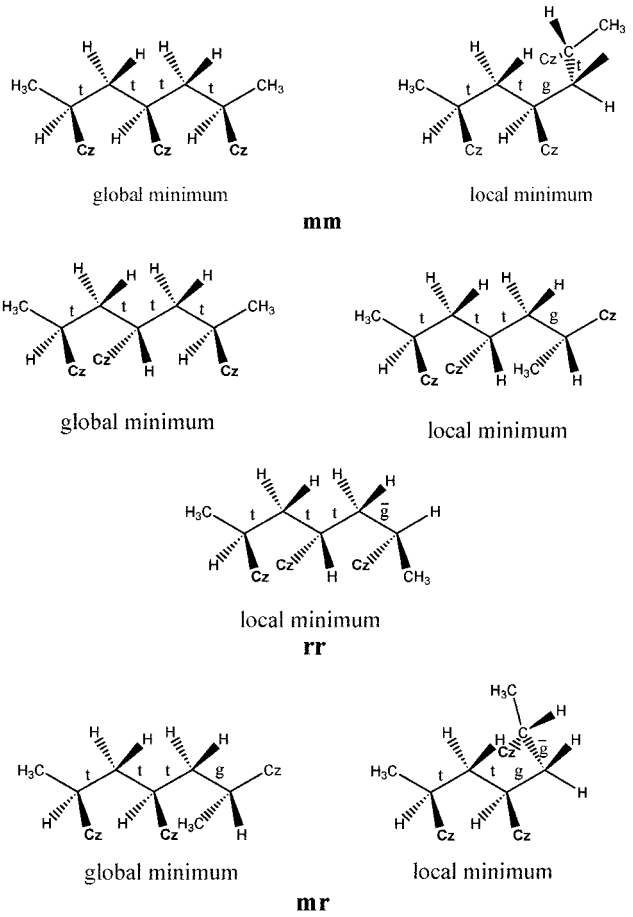

Figure 5. Lowest energy conformations for the *meso*, *racemic*, and *hetero* trimers corresponding to the isotactic (mm), syndiotactic (rr), and heterotactic (mr) triads, respectively.

conformational energies (the energy of the lowest minimum for each trimer is assigned arbitrarily to zero), the populations, and the bond conformations in each trimer are summarized in Table 1.

Similar calculations were also performed upon rotation around the penultimate bonds in the trimers (Figure 1b). The conformational energy maps obtained from these calculations

Table 1. Conformational Energies (kcal mol^{-1}), Stereochemical Arrangements, and Relative Populations[a] in Each Trimer, Corresponding to Isotactic (mm), Syndiotactic (rr), and Heterotactic (mr) Sequences

conformers	stereochemical arrangement	energy (kcal mol^{-1})	population (%)
	Isotactic (mm)		
1	tttt	0.00	20.15
2	ttgt	4.89	0.01
3	tgtt	4.73	0.01
	Syndiotactic (rr)		
1	tttt	0.00	29.18
2	tttg	2.83	0.27
3	ttt $\bar{g}$	2.16	0.80
	Heterotactic (mr)		
1	tttg	0.00	49.48
2	ttg $\bar{g}$	5.14	0.01
3	$\bar{g}$gtt	5.20	0.01

[a] Weighted by the appropriate Bernoulli probability (see text).

showed only minor differences from those described previously. Therefore, information obtained from the conformational analysis assuming rotations around the central bonds of the trimer will be used to compare model structures with those obtained from the NOESY experiments.

Calculation of the Relaxation Matrix. The time dependence of the cross-peaks in the NOESY spectrum is given by eq 1:[15,21]

$$\mathbf{V}(\tau_m) = \mathbf{V}_0 \exp(-\mathbf{R}\tau_m) \quad (1)$$

where $\mathbf{V}(\tau_m)$ is the peak-volume matrix at the mixing time τ_m, $\mathbf{V}_0$ is the peak-volume matrix at zero mixing time, and $\mathbf{R}$ is the relaxation rate matrix containing the cross-relaxation rates as off-diagonal elements and the longitudinal decay rates as the diagonal elements. The cross-relaxation rate for protons i and j is given by

$$\sigma_{ij} = \frac{1}{10}\left(\frac{\gamma^2\hbar}{r_{ij}^3}\right)^2\{-J_0(0) + 6J_2(2\omega)\} \quad (2)$$

where γ and ω are the gyromagnetic ratio and the Larmor frequency of protons, and r_{ij} is the inter-proton distance. For isotropic motion described by the molecular correlation time τ_C, the spectral densities have the form

$$J(n\omega) = \frac{2\tau_C}{1 + (n\omega)^2\tau_C^2} \quad (3)$$

Since cross-relaxation rates depend on the interpoton distance and correlation time through eqs 2 and 3, NOESY experiments can be used to determine the dynamics and internuclear distances.

The approach used here is to simulate the experimental NOESY spectrum, i.e., the peak volumes $\mathbf{V}(\tau_m)$ and $\mathbf{V}_0$, from a model structure using the program CORMA.[16] Comparison between measured volumes and volumes calculated from the proposed structure allows an assessment of the validity of the model structure. The simulation of NOESY volumes with CORMA is based on the ensemble averaged relaxation rates over the number of conformers resulting from the conformational analysis. Conformations corresponding to the energy minima in the conformational energy map of each trimer (Figures 2−4) were taken into account in the averaging procedure of these calculations. The relative population P_i of each conformer i within each trimer with energy E_i, distributed over n conformational states, has been calculated by a Boltzmann distribution,

$$P_i = \exp(-E_i/k_BT)/\sum_n \exp(-E_i/k_BT) \quad (4)$$

where k_B is Boltzmann's constant. The population of each conformer in a given trimer must be weighted by the pertinent probability of each triad sequence [*meso* (mm), *racemic* (rr), and *hetero* (mr)], which appears in the PNVC chain. From the aliphatic ^{13}C NMR spectrum a *meso* probability, $P_{iso} = 0.49$, for the addition of *meso* (isotactic) dyad was estimated for the commercial polymer by employing Bernoullian statistics. This value is very close to that obtained in the literature[11] ($P_{iso} = 0.45$) for the PNVC polymer obtained from the same source. Following Bernoullian statistics, the population of the various conformers in the isotactic trimer was multiplied by P_{iso}^2, the syndiotactic trimer by $(1 - P_{iso})^2$, and the heterotactic trimer by $2P_{iso}(1 - P_{iso})$.

Results and Discussion

Conformational Energies for the Dimers. Conformational energy maps for internal bond rotation on the dimer model compounds of PNVC and *meso* and *racemic* 2,4-dicarbazolylpentane have been reported in the literature.[6,10,22,23] Nevertheless, the estimated conformational energies and in particular the populations of the various conformers in each dimer appear to depend strongly on the semiempirical energy functions used in these calculations.[6] Since our approach for constructing conformational energy contour maps uses semiempirical energy expressions that differ from those employed in the past, it is important to check the validity of our calculations against the older results. In this respect, we performed conformational energy calculations for the dimer model compounds, *meso* and *racemic* 2,4-dicarbazolylpentane, by employing the energy expressions of the MM$^+$ molecular mechanics program, presented previously. The results of our analysis on *meso* and *racemic* 2,4-dicarbazolylpentane show the same trends as observed in other studies. The minimum-energy conformer for the *meso* 2,4-dicarbazolylpentane was the tt state, whereas the relative energies of the tg and tg states were higher by 1.7 and 1.6 kcal mol^{-1}, respectively. For the *racemic* 2,4-dicarbazolylpentane, the tt state was characterized with the lowest energy. The other two minimum-energy states, gt and gg, were characterized with higher relative energies of 0.8 and 0.55 kcal mol^{-1}, respectively. However, it should be noted that energy minimization performed on the *meso* dimer by using the semiempirical PM3 program led to the gt state as the minimum-energy conformation.

NOESY Volumes. Figure 6 illustrates the experimental 500 MHz NOESY spectrum of **1** in chloroform solution at 303 K with mixing time 450 ms. The one-dimensional NMR spectrum of the aromatic protons has been assigned previously.[24] The NOESY spectrum shows several cross-peaks between aromatic protons of the carbazole group, between aliphatic protons of the polymer backbone (CH and CH_2), and more interestingly between aliphatic and aromatic protons. In particular, cross-peaks of various intensities connect the backbone aliphatic protons with the aromatic protons H-1 and H-8. A number of cross-peaks, especially between aromatic protons, show severe overlaps. In this case, estimated volumes for the overlapping peaks can be used in combination with the measured peak volumes for the resolved peaks in the spectrum. However, this approach is not exact because the simulation of the overlapping peaks is not unique, although the peak volume vs mixing time simulations using the complete relaxation rate matrix are expected to be more accurate than those obtained using the initial rate approximation (ISPA). The simulations of the cross-peak volumes for

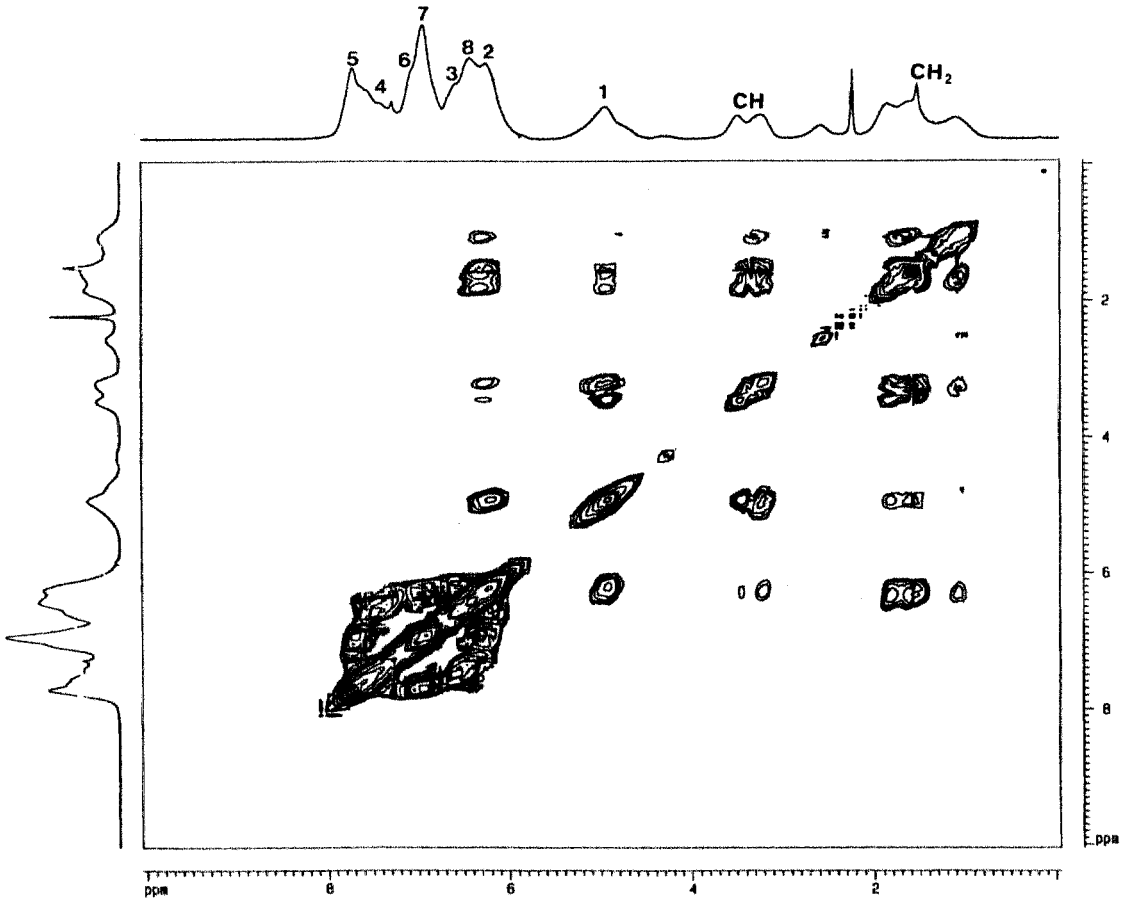

Figure 6. The 500 MHz NOESY spectrum of poly(*N*-vinylcarbazole) obtained with mixing time 450 ms at 30 °C.

Table 2. Normalized Experimental and Theoretical (in Parentheses) Cross-Peak Volumes for NOESY Spectra of PNVC at Several Mixing Times

mixing time (ms)	H-1−H-2	H-1−CH	H-1−CH_2	H-8−CH	H-8−CH_2	CH−CH_2
50	0.005 (0.014)	0.009 (0.006)			0.011 (0.009)	0.028 (0.025)
100	0.012 (0.016)	0.025 (0.014)			0.014 (0.016)	0.057 (0.049)
150	0.024 (0.024)	0.028 (0.018)	0.003 (0.023)	0.004 (0.005)	0.027 (0.023)	0.056 (0.058)
250	0.032 (0.037)	0.041 (0.031)	0.030 (0.019)	0.008 (0.008)	0.027 (0.033)	0.066 (0.070)
350	0.038 (0.050)	0.045 (0.038)	0.046 (0.026)	0.028 (0.011)	0.056 (0.047)	0.086 (0.095)
450	0.028 (0.060)	0.065 (0.046)	0.055 (0.029)	0.015 (0.013)	0.050 (0.047)	0.085 (0.111)
550	0.033 (0.070)	0.076 (0.051)	0.064 (0.029)	0.027 (0.014)	0.082 (0.054)	0.063 (0.115)
650	0.045 (0.078)	0.069 (0.055)	0.056 (0.025)	0.033 (0.016)	0.108 (0.056)	0.065 (0.129)
750	0.060 (0.085)	0.057 (0.057)	0.052 (0.035)	0.034 (0.018)	0.111 (0.057)	0.046 (0.126)

the protons of interest in the NOESY spectrum of Figure 6, as well as those obtained at mixing times mentioned in the experimental part, are summarized in Table 2. The simulated cross-peaks among those aromatic protons, which show severe overlaps, are not included in Table 2. These values are not considered to be significantly reliable. The experimental volumes were normalized with respect to the calculated absolute values. Normalization was performed through the following normalization factor incorporated in CORMA:

$$f_{\text{norm}} = \frac{\sum_i V_c(i)}{\sum_i V_e(i)} \tag{5}$$

where $V_c(i)$ and $V_e(i)$ are the volumes of the calculated and experimental cross-peaks i in the NOESY spectra for a particular structure. From Table 2, it can be seen that the normalized experimental volumes are generally in good agreement with the theoretical values, indicating that the calculations are reasonably realistic. In most cases, the discrepancy between calculated and experimental volumes is much less than the experimental error (20−30%) involved in the determination of the peak-volume matrix. It is worth noting that the calculated distance (2.6 Å) between protons H-1 and H-2, which are located in the rigid carbazole ring, and hence correspond to a fixed distance, from their cross-peak volumes was found to be very close to the value obtained upon geometry optimization (2.5 Å).

The match of theoretical to experimental data is also reflected by the quality factors R and R^x incorporated in CORMA. The R factor is equivalent to the crystallographic R factor, and R^x is a variation of the R factor involving sixth-root weighting of volumes to avoid domination by short relaxation pathways,[25,26] that is

$$R^x = \sum_i |V_e^{1/6}(i) - V_c^{1/6}(i)| / \sum_i |V_e^{1/6}(i)| \tag{6}$$

For the calculated volumes of the various structures of trimers and with the mixing times used in this study,

the R factor ranged from 0.03 to 0.467 and the R^x factor from 0.01 to 0.336. The satisfying simulation of the experimental cross-peak volumes of the NOESY spectra indicates that the model structures used in these calculations represent a good choice for the conformational behavior of PNVC.

Overall and Internal Motions in PNVC Chain. One of the major difficulties in reproducing the theoretical NOESY volumes for flexible molecules using the complete relaxation matrix analysis (CORMA) is the evaluation of the various correlation times describing overall and internal motions, which affect the cross-relaxation rates (eq 2). Usually, molecular correlation times describing the various modes of reorientation can be obtained from ^{13}C NMR spin−lattice relaxation measurements in combination with dynamic modeling.[27] Such a treatment has been undertaken for PNVC in dilute solutions.[5] Local chain dynamics of PNVC were described by a bimodal time-correlation function developed by Dejean, Laupretre, and Monnerie[28] (DLM). The correlation times describing isolated single conformational transition and cooperative conformational transitions of the *trans*−*gauche* type were found to be $\tau_0 =$ 23.2 ns and $\tau_1 = 1.16$ ns, respectively, in chloroform at 30 °C.[5] A third type of chain local motion considered in this model is the librational motion of the backbone C−H vector about the rest position of the C−H bond. This motion occurs freely within a cone of half-angle θ with correlation time τ_2. In chloroform at 30 °C, τ_2 was found to be 4.14 ps, while the angle θ, which is temperature-independent, was found to be 22.5° and 26° for the C−H vectors at the methine and methylene carbon sites of PNVC, respectively. As mentioned previously, the internal rotation of the carbazole ring is highly restricted and has not been taken into consideration in the calculations.

However, the previously mentioned DLM time-correlation function used to describe the segmental motions of PNVC cannot be incorporated into the CORMA program without substantial modifications. CORMA calculates spectral densities in the form of the model-free approach developed by Lipari and Szabo.[29] The complete spectral density function of the model-free approach, $J(\omega,A,S^2,\tau'_1,\tau'_2,\tau_e)$, incorporates the correlation times, τ'_1 and τ'_2, describing anisotropic overall motion, the correlation time, τ_e, describing internal motion, the Larmor frequency, ω, the anisotropy factor, A, and the generalized order parameter, S^2. In the program, the ratio τ'_1/τ'_2 is specified. For $\tau'_1/\tau'_2 = 1$, or $A = 1$, isotropic motion is considered. If $S^2 = 1$, then internal motion is ignored. If both A and S^2 are set to one, isotropic motion with no internal rotation is considered. It should be noted that the model-free approach should comply with the following rules in order to be valid.[28] First, the internal motions should be much faster than the overall motion and, second, should occur within the extreme motional narrowing limit.

Considering the trimer model structures, we performed the full relaxation matrix analysis by adopting the isotropic motional model with internal rotation the librational motion of the C−H vector mentioned previously. Accordingly, we calculated the parameter S^2 for the overall and internal motions using the spectral density function of the model-free approach and keeping $\tau'_1 = \tau'_2 = \tau_1 = 1.16$ ns and $\tau_e = \tau_2 = 4.14$ ps. The input parameters for CORMA regarding rates of motion were $\tau'_1/\tau'_2 = 1$ (or $A = 1$), $S^2 = 0.616$, and the values of τ'_1 and τ_e.

The choice of the DLM motional parameters for the present calculations is based on the following arguments: (1) For this high molecular weight polymer ($M_w = 10^6$), chain segmental motion is the dominant relaxation source, while overall molecular reorientation of the polymer chain is too slow to affect significantly the dipole−dipole relaxation and hence the NOESY volumes. (2) The segmental motion, which comprises a few monomer units, reflects in a satisfactory manner the time scale of the motion of the trimers; depending on the polymer structure, motional cooperativity is restricted within a polymer segment involving 1−3 monomer units.[27] (3) Internal motion of the carbazole group is highly restricted as mentioned earlier.

Bond Conformations and Excimer Formation. It is interesting to compare the global and local energy minima of the conformational energy maps of the three model structures (Figures 2−4 and Table 1), corresponding to (mm), (rr), and (mr) triad sequences of the polymer microstructure, in relation to the bond conformational arrangements. In the isotactic triad of five skeletal carbons, the lowest energy (global minimum) corresponds to the state tttt, whereas the other two states correspond to ttgt and tgtt conformations, which are characterized by higher energies (Table 1). Also, the populations of the higher energy states are the same and much lower than the population of bond conformation of the global minimum. Such a large difference in energy, in favor of the tttt conformation, has been attributed to the contribution of small attractive energies between several pairs of interacting atoms of the carbazole groups in the *all-trans* conformation.[10]

The global minimum in the syndiotactic triad corresponds to the tttt conformation of the five skeletal bonds. However, a higher population than the corresponding conformation of the isotactic triad characterizes the tttt bond conformation of the syndiotactic triad. The energies and the populations of other two conformational states, tttg and ttt$\bar{g}$, are not the same. The energy of the tttg conformation is about 0.6 kcal mol^{-1} higher than that of the ttt$\bar{g}$ state. In addition, the population of the former state is about 3 times smaller than that of the latter state. An explanation of this difference can be given by inspection of the bond conformations depicted in Figure 5 for the syndiotactic triad. Contrary to the tttg conformation, which favors one partial overlap between two neighboring carbazole groups, the ttt$\bar{g}$ conformation favors one partial and two full overlaps between three rings, thus increasing the small attractive forces between several pairs of interacting atoms of the carbazole groups.

An increase in the gauche states is observed for the heterotactic triad. As expected, conformation such as ttg$\bar{g}$ and $\bar{g}$gtt are characterized by the highest energies across the potential energy surface. The global minimum in the heterotactic triad corresponds to the state tttg and is characterized by the largest population. It is worth noting that the populations of the bond conformations corresponding to the global minima within each trimer follow the same order of the concentrations of each triad sequence in the polymer chain.

These results indicate clearly that bond conformation, such as tttt occurs in both the isotactic and syndiotactic triads, whereas conformation tttg is common for the syndiotactic and heterotactic triads. This observation is important for the type of the excimer formed in each triad sequence. The tttt conformation in the isotactic

triad favors the formation of the true excimer, inasmuch as the neighboring carbazole rings adopt the proper parallel orientations. On the other hand, the tttt conformation in the syndiotactic triad appears to support the formation of the second excimer. In this conformation, it seems easy for one of the two benzene rings of the bulky carbazole moiety to approach and mutually overlap one benzene ring of the neighboring carbazole chromophore.

The other conformations of the trimers characterized by higher energies (Figure 5) favor the formation of either the true excimer or the second excimer, but these are confined within dyad sequences.

Comparison with Other Calculations. There are numerous studies[13−15] in the past using NOESY experiments in conjunction with various calculation strategies to generate structures for biomacromolecular systems (e.g., proteins, nucleic acids, oligo- and polysaccharides). However, this methodology has found scarce application toward conformational properties of synthetic polymers. To the best of our knowledge, one such study has appeared in the literature. The group at AT&T Bell Laboratories has used NOESY experiments to study the solution conformation of a strictly alternating styrene−methyl methacrylate copolymer.[30,31] However, a different computational approach than ours has been attempted to measure the dipolar interactions between protons. Instead of calculating NOESY cross-peak volumes for feasible model structures and comparing the calculated volumes with experimental ones (analysis with CORMA), they have used the so-called direct method. In this approach, the elements (diagonal and cross-relaxation rates) of the relaxation matrix have been calculated from the diagonal and cross-peak volumes of the NOESY spectra through eq 7 obtained upon diagonalization of eq 1[31]

$$\frac{\chi \ln \mathbf{D} \chi^{-1}}{\tau_m} = \mathbf{R} \tag{7}$$

Here, χ is the matrix of the eigenvectors and $\mathbf{D}$ the diagonal matrix of eigenvalues of $\ln[\mathbf{V}(\tau_m)/\mathbf{V}_0]$. The volumes of the diagonal peaks at various mixing times were extrapolated to zero mixing time to obtain $\mathbf{V}_0$. The calculated cross-relaxation rates were converted into inter-proton distances using the fixed geminal inter-proton distance as an internal reference[31]

$$\frac{\sigma_{ij}}{\sigma_{gem}} = \frac{r_{ij}^{-6}}{r_{gem}^{-6}} \tag{8}$$

where r_{gem} and r_{ij} are the geminal and unknown proton distances and σ_{gem} and σ_{ij} are the corresponding cross-relaxation rates. Equation 8 assumes that the dynamics of all the protons are similar, thus factoring out the spectral densities (and correlation times) incorporated in eq 2. Finally, the constraints imposed by the measured inter-proton distances were used to determine the average solution conformation of the styrene units in the coheterotriads of the copolymer.

This direct method is clearly ideal for distance determination provided that the molecule yields spectra with very high signal-to-noise ratio, in which most of the major peaks are well resolved and the volumes are accurately estimated. Also, this approach is model-independent and does not require a priori knowledge of correlation times describing internal motions. Nevertheless, this method cannot be used in the present study due to two complications. The first is related to the low-resolution NOESY spectra of the PNVC polymer, which prohibit the extraction of accurate diagonal peak volumes for protons located in the rigid carbazole segments of the molecule. Severe diagonal peak overlaps are observed in the aromatic region (protons H-2 to H-8) of the NOESY spectra (Figure 6). Second, tacticity effects do not allow a clear separation of the diagonal peaks of the geminal backbone CH_2 protons. These limitations prevent the calculation of the reference cross-relaxation rate (e.g., between protons H-1 and H-2 and/or between geminal protons of the backbone CH_2 group) and thus calculation of distances through eq 8.

Conclusion

The present study demonstrates that combining CORMA-derived volumes, calculated from model structures based on triad stereochemical sequences of PNVC, is an effective method to determine the conformational behavior of this important polymer in solution. Also, this study demonstrates that previous conclusions regarding the photophysical behavior of PNVC cannot be based solely on the conformations of the *meso* and *racemic* dyads but rather on larger stereochemical sequences reflecting the conformational behavior of real chains.

Acknowledgment. We gratefully acknowledge financial support from the General Secretariat for Research and Technology of Greece, the British Council, and NATO (Grant CRG 9600593).

References and Notes

(1) Block, H. *Adv. Polym. Sci.* **1979**, *33*, 93.
(2) Johnson, G. E. *J. Chem. Phys.* **1975**, *62*, 4697.
(3) Itaya, A.; Okamoto, K.; Kusabayashi, S. *Bull. Chem. Soc. Jpn.* **1976**, *49*, 2082.
(4) Sakai, H.; Itaya, A.; Masuhara, H.; Sasaki, K.; Kawata, S. *Polymer* **1996**, *37*, 31.
(5) Karali, A.; Dais, P.; Heatley, F. *Macromolecules* **2000**, *33*, 5524.
(6) Abe, A.; Kobayashi, H.; Kawamura, T.; Date, M.; Uryu, T.; Matsuzaki, K. *Macromolecules* **1988**, *21*, 3414.
(7) Vandendriessche, J.; Palmans, P.; Toppet, S.; Boens, N.; De Schryver, F. C.; Masuhara, H. *J. Am. Chem. Soc.* **1984**, *106*, 8057.
(8) De Schryver, F. C.; Vandendriessche, J.; Toppet, S.; Demeyer, K.; Boens, N. *Macromolecules* **1982**, *15*, 406.
(9) Evers, F.; Kobs, K.; Memming, R.; Terrel, D. R. *J. Am. Chem. Soc.* **1983**, *105*, 5988.
(10) Sundararayan, P. R. *Macromolecules* **1980**, *13*, 512.
(11) Natansohn, A. *J. Polym. Sci., Polym. Chem.* **1989**, *27*, 4257.
(12) Kawamura, T.; Matsuzaki, K. *Makromol. Chem.* **1978**, *179*, 1003.
(13) James, T. L.; Basus, V. J. *Annu. Rev. Phys. Chem.* **1991**, *42*, 501.
(14) Borgias, B. A.; James, T. L. In *Biological Magnetic Resonance*; Berliner, L. J., Reuben, J., Eds.; Plennum Press: New York, 1990; Vol. 9, pp 119−154.
(15) Keepers, J. W.; James, T. L. *J. Magn. Reson.* **1984**, *57*, 404.
(16) Borgias, B. A.; Thomas, P. D.; James, T. L. Complete Relaxation Matrix Analysis (CORMA), University of California, San Francisco, 1992.
(17) Gronenborn, A. M.; Clore, G. M. *Prog. Magn. Reson. Spectrosc.* **1985**, *20*, 1.
(18) James, T. L.; Borgias, B. A.; Bianucci, A. M.; Zhou, N. In *NMR Application in Biopolymers*; Finley, W., Schmidt, S. J., Serianni, A. S., Eds.; Plenum Press: New York, 1990; pp 135−154.
(19) Macura, S.; Huang, Y.; Suter, D.; Ernst, R. R. *J. Magn. Reson.* **1981**, *43*, 259.
(20) HyperChem 5.1, Hypercube Inc. Gainesville, FL, 1998.
(21) Jeener, J.; Meier, B. H.; Bachmann, B.; Ernst, R. R. *J. Chem. Phys.* **1979**, *71*, 4546.

(22) Molina, M. S.; Baraales-Rienda, J. M.; Riande, E. *Macromolecules* **1984**, *17*, 2728.
(23) Privratska, J.; Havranek, A. *Acta Polym*. **1980**, *31*, 130.
(24) Karali, A.; Frudakis, G.; Dais, P.; Heatley, F. *Macromolecules* **2000**, *33*, 3180.
(25) Gonzalez, C.; Rullmann, J. A. C.; Bonvin, A. M. J. J.; Boelens, R.; Kaptein, R. *J. Magn. Reson*. **1991**, *91*, 659.
(26) Schmitz, U.; Kumar, A.; James, T. L. *J. Am. Chem. Soc*. **1992**, *114*, 10654.
(27) Dais, P.; Spyros, A. *Prog. NMR Spectrosc*. **1995**, *27*, 555.
(28) Dejean de la Batie, R.; Laupretre, F.; Monnerie, L. *Macromolecules* **1988**, *21*, 2045.
(29) Lipari, G.; Szabo, A. *J. Am. Chem. Soc*. **1982**, *104*, 4546.
(30) Heffner, S. A.; Bovey, F. A.; Verge, L. A.; Mirau, P. A.; Tonelli, A. E. *Macromolecules* **1986**, *19*, 1628.
(31) Mirau, P. A.; Bovey, F. A.; Tonelli, A. E.; Heffner, S. A. *Macromolecules* **1987**, *20*, 1701.

MA010117N